

PAPER

## Nonlinear absorption properties of silicene nanosheets

To cite this article: Fang Zhang *et al* 2018 *Nanotechnology* **29** 225701

View the [article online](#) for updates and enhancements.

### You may also like



- [Analysis of multi-photon absorption: z-scan using ultra-short Gaussian vortex beam](#)  
Srinivasa Rao Allam
- [High-performance two-photon absorption optical limiter and stabilizer based on phase-pure thick-shell CdSe/CdS core/shell quantum dots](#)  
Chen Liao, Zhiwei Peng, Luping Tang et al.
- [Two-photon absorption in colloidal semiconductor nanocrystals: a review](#)  
Arthur Alo, Jonathan C Lemus, Claudevan A Sousa et al.



**ECS**  
The  
Electrochemical  
Society  
Advancing solid state &  
electrochemical science & technology

**DISCOVER**  
how sustainability  
intersects with  
electrochemistry & solid  
state science research

# Nonlinear absorption properties of silicene nanosheets

Fang Zhang<sup>1</sup> , Mengxia Wang<sup>2</sup> , Zhengping Wang<sup>2</sup>, Kezhen Han<sup>1</sup>, Xiaojuan Liu<sup>1</sup> and Xinguang Xu<sup>2</sup>

<sup>1</sup> School of Physics and Optoelectronic Engineering, Shandong University of Technology, Zibo, 255000, People's Republic of China

<sup>2</sup> State Key Laboratory of Crystal Materials, Shandong University, Jinan, 250100, People's Republic of China

E-mail: [yourszhangfang1988@126.com](mailto:yourszhangfang1988@126.com)

Received 20 January 2018, revised 23 February 2018

Accepted for publication 14 March 2018

Published 29 March 2018



## Abstract

As the cousins of graphene, i.e. same group IVA element, the nonlinear absorption (NLA) properties of silicene nanosheets were rarely studied. In this paper, we successfully exfoliated the two-dimensional silicene nanosheets from bulk silicon crystal using liquid phase exfoliation method. The NLA properties of silicene nanosheets were systemically investigated for the first time, as we have known. Silicene performed exciting saturable absorption and two photon absorption (2PA) behavior. The lower saturable intensity and larger 2PA coefficient at 532 nm excitation indicates that silicene has potential application in ultrafast lasers and optical limiting devices, especially in visible waveband.

Keywords: silicene nanosheets, nonlinear absorption, saturable absorption, optical limiting

(Some figures may appear in colour only in the online journal)

## 1. Introduction

On account of the high charge mobility and intrinsic zero band gap structure [1], two-dimensional (2D) structure graphene refreshed the traditional viewpoints on nano-materials [2]. The other 2D materials, such as MoS<sub>2</sub>, MoSe<sub>2</sub>, WS<sub>2</sub>, WSe<sub>2</sub>, phosphorene, boron nitride and antimonene have caught people's intense interest for their unique chemical, electronic and optical properties [3–6].

Si occupies a crucial position in modern electronic technology. Due to its size-quantization effects, low-dimensional silicon is an encouraging candidates for applications in photonic and electronic devices [7–9]. Extensive research has been based on the synthesis and processing of silicon quantum dots, silicon nanowires and 2D allotropic forms [10–12]. Up to now, buckled 2D silicene structures have been synthesized on substrates with a metallic character, such as Ag(111) [13–15], Ir(111) [16] and ZrB<sub>2</sub> [17]. In 2011, Lu *et al* developed a facile method to synthesize ultrathin silicene nanosheets using graphene oxide as the sacrificial template [18]. In 2014, Kim *et al* reported the dendritic gas-phase 2D growth of silicene with 1–13 nm thickness [19]. In 2016, Ryu

*et al* synthesized high quality silicene nanosheets with 5 nm thickness utilizing natural clays [9].

Most 2D materials exhibit exciting nonlinear absorption (NLA) properties [20–25] and have promising applications in the optical field. Considering their saturable absorption (SA) properties, 2D materials can be used as saturable absorbers applied in all-solid-state Q-switched and mode-locked ultrafast lasers [26–28]. For the two photon absorption (2PA) behavior, the 2D materials can act as optical limiting (OL) materials to protect the human eye and the sensitive optical component from laser-induced damage [21]. Until now, research on the NLA properties of silicene nanosheets is very scarce, which deeply restricts its application in optics.

In this paper, adopting the liquid phase exfoliation (LPE) method, we successfully exfoliated the 2D silicene nanosheets from bulk silicon crystal. At the same time, the NLA properties of the silicene nanosheets were systemically researched using open aperture *z*-scan technique. The SA performance and OL behavior were simultaneously observed. The results demonstrate that silicene nanosheets have exciting NLA properties. The low saturable intensity and high 2PA coefficient demonstrates silicene is a promising NLA material.

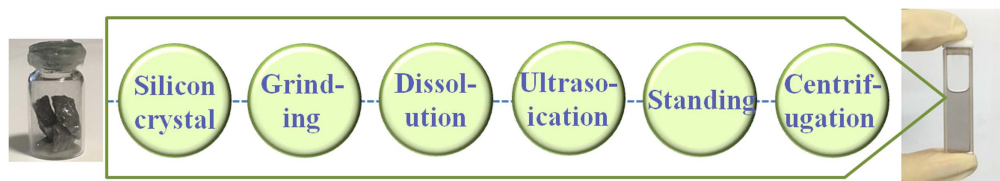


**Figure 1.** Preparation processes of silicene nanosheets.

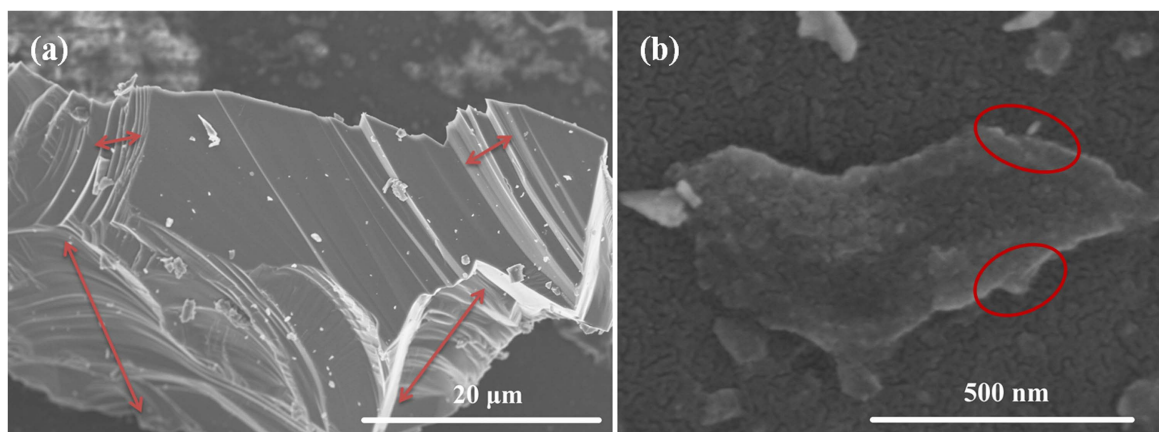


**Figure 2.** SEM image of (a) silicon crystal and (b) prepared silicene nanosheets.

## 2. Sample preparation

LPE is an effective and straightforward method to produce high-quality 2D nanosheets from layered bulk crystals [29, 30]. The silicene nanosheets were manufactured using the LPE method assisted with sonication. Considering the on-surface isolation, no surfactant was required in the exfoliation process. Due to the hypotoxicity, ultra pure ethanol was selected as the organic solvent. Figure 1 shows the preparation process of the silicene nanosheets combining with the images of original silicon crystals and prepared silicene nanosheets. The silicon crystals are black and have a metallic luster. Using an agate mortar, the silicon crystals were grinded for hours for the generation of nanosheets. During the grinding process, small amounts of alcohol were added to protect the sample from oxidization. At the same time, the small amounts of alcohol had the function of lubrication. The grinded powder was dissolved in ethanol. In order to effectively exfoliate the silicene nanosheets, a sonication (40 KHz frequency) was carried out for 3 h to reduce the interaction between nanosheets and disperse the produced nanosheets. The prepared dispersion liquid was settled for 36 h for precipitating the large silicon grains. After centrifugation for 30 min with a speed of 1500 rpm, the dispersion liquid became stratified. The top one fifth of the dispersion liquid was collected as the experiment sample and stored in a quartz colorimetric utensil with 2 mm thickness. The sample concentration was estimated to be  $50 \text{ mg l}^{-1}$ . With the observation of naked eyes, the sample was not precipitated during the nonlinear experiment process, which can be estimated that the concentration of dispersion liquid was almost in the same level throughout the experiment process.

## 3. Characterization

A scanning electron microscope (SEM, S-4800, Hitachi Japan) was used to observe the morphology of the silicon crystal and exfoliated silicene nanosheets. The SEM image of the silicon crystal is shown in figure 2(a). It looks very smooth at the surface of each layer. Silicon is apparently stratified at the edge of crystal (red arrows), which indicates the samples can be effectively exfoliated using LPE or mechanical exfoliation methods. The surface appearance of silicene nanosheets is displayed in figure 2(b). At the edge of the silicene, the few-layer structure can be identified (red circle).

The atomic force microscopy (Dimension Icon, Veeco Instruments Inc.) with peak force tapping mode was used to measure the thickness of silicene. Figures 3(a) and (b) indicate the step heights of typical silicene nanosheets. The heights are in the range of 4.5–8.5 nm, i.e. around 14–27 layers [9]. The small bright spot on the sample might be caused by the accumulation of small nanosheets. Nevertheless, due to the un-evaporated solvent and the adhesion forces of samples, the measured heights of the layered samples prepared by LPE are easily overestimated. Therefore, the actual thicknesses of the silicene nanosheets might be smaller.

The linear absorption coefficient of silicene can be determined by the transmission spectrum (UV–vis spectrophotometer, Cary 50, VARIAN Company, America). Figure 3(c) shows the transmission spectrum of the silicene nanosheets with a spectral range of 250–1130 nm. The broadband absorption predicts the broadband absorption material of the silicene nanosheets. By measuring the transmittance  $T$  of silicene dispersion liquid plus quartz colorimetric utensil, and  $T_0$  of ethanol plus quartz

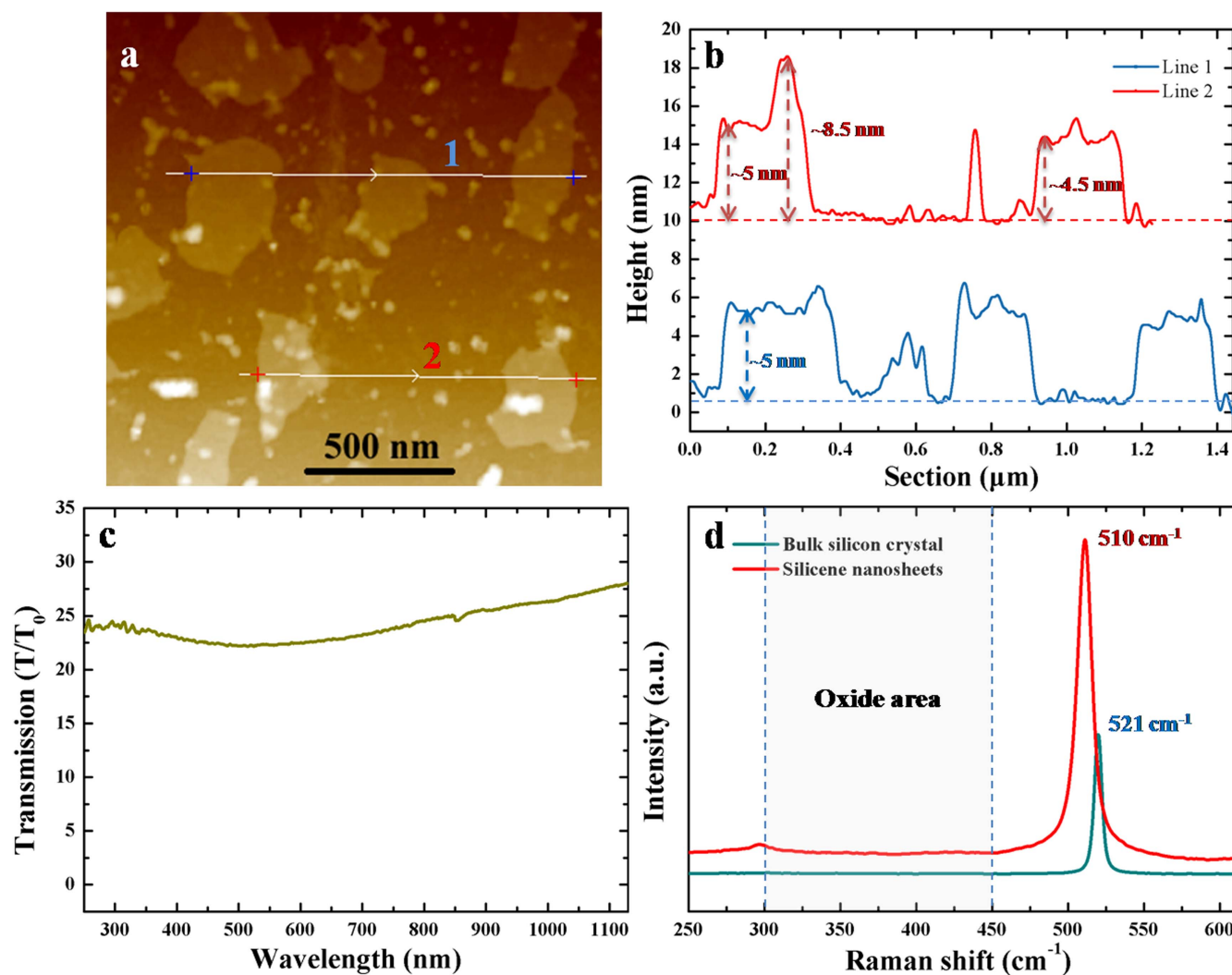


**Figure 3.** (a) AFM image of silicene nanosheets, (b) corresponding heights of sample, (c) transmission spectrum of silicene nanosheets, and (d) Raman spectra of silicon crystal and the prepared silicene nanosheets.

colorimetric utensil, the transmittance  $T/T_0$  of the silicene nanosheets at  $50 \text{ mg l}^{-1}$  concentration can be obtained. The transmittances at 1064 and 532 nm are 27.17% and 22.31%, respectively. The linear absorption coefficients  $\alpha_0$  at 1064 and 532 nm are calculated to be  $6.5$  and  $7.5 \text{ cm}^{-1}$ , respectively, adopting the equation  $T_{\text{abs}} = \exp(-\alpha_0 L)$ , where  $T_{\text{abs}} = T/T_0$  and  $L = 2 \text{ mm}$ .

In order to reflect the structure and quality of the nanomaterials, Raman spectroscopy was carried out. Figure 3(d) displays the Raman spectra of the bulk silicon crystal and silicene nanosheets using a Raman spectrometer (LabRAM HR800, HORIBA Ltd). Bulk silicon crystal owns one sharp peak at  $521 \text{ cm}^{-1}$  originating from the microcrystalline [31]. The intense Raman peak of the silicene nanosheets is at  $510 \text{ cm}^{-1}$  with widened full width at half maximum and a visible shift to a lower frequency ( $11 \text{ cm}^{-1}$ ), which shows that the nanosheets were efficiently exfoliated at a height of around  $5 \text{ nm}$  [32–36]. In addition, peaks caused by amorphous surface oxides around  $300\text{--}450 \text{ cm}^{-1}$  and the peak at  $480 \text{ cm}^{-1}$  caused by amorphous Si were not observed, which indicates the high purity of the silicene nanosheets [9].

#### 4. NLA experiment

Adopting an open aperture Z-scan technique, the NLA response of the as-prepared silicene dispersion liquid was investigated. The excitation wavelengths are 1064 and 532 nm with pulse width of 40 and 30 ps, respectively. The laser repetition rate is 10 Hz. The focal length of the convex lens is 30 cm.

Figure 4 displays the measurement results of the silicene nanosheets, which manifest exciting NLA properties of silicene. When the excitation energy reaching the threshold of the NLA, the normalized transmittance increased with the excitation intensity increasing and formed a peak at the focus location (figures 4(a<sub>1</sub>), (b<sub>1</sub>)). The silicene nanosheets exhibited SA, i.e. single photon absorption (1PA). If further increasing the excitation energy, the SA behavior became saturated and the OL behavior (caused by 2PA behavior) appeared, which caused a rapid decline of transmittance and formed a trough at the focus location (figures 4(a<sub>2</sub>), (b<sub>2</sub>)). When the excitation energy continually augmented, the SA was strongly suppressed and the OL behavior held dominant



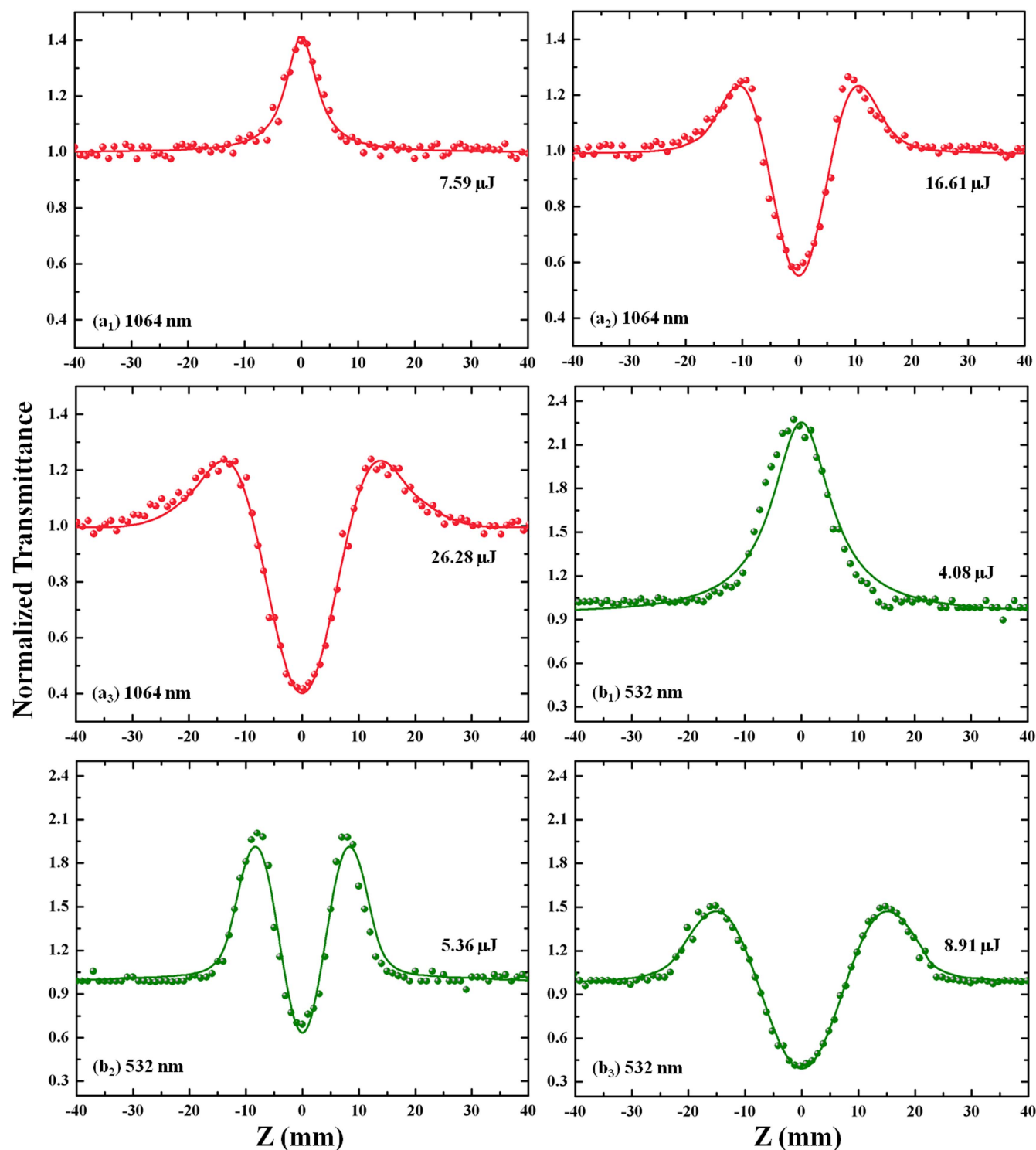


**Figure 4.** Open-aperture Z-scan results of silicene nanosheets with excitation of (a) 1064 and (b) 532 nm wavelengths at different excitation intensities (the points are the experimental data and the solid lines are the fitted curves).

position (figures 4(a<sub>3</sub>), (b<sub>3</sub>)). For 1064 nm excitation, the maximum normalized transmittance of SA and the strongest OL modulation depth were 140% and 60%, with 7.59 and 26.28  $\mu\text{J}$  excitation, respectively. For a 532 nm excitation, they were 226% and 61% with 4.08 and 8.91  $\mu\text{J}$  excitation, respectively. If further augmenting the excitation intensity was to occur, a stronger OL behavior would be seen. The

normalized transmittance of pure solvent was maintained at the same value (constant 1) when  $Z$  changed from  $-40$  to  $40$  nm, which means that no nonlinear effects occurred in pure solvent.

Figure 5(a) exhibits the relationship between normalized transmittance and excitation intensity of 1064 and 532 nm excitation, which is transformed from figures 4(a<sub>3</sub>) and (b<sub>3</sub>).

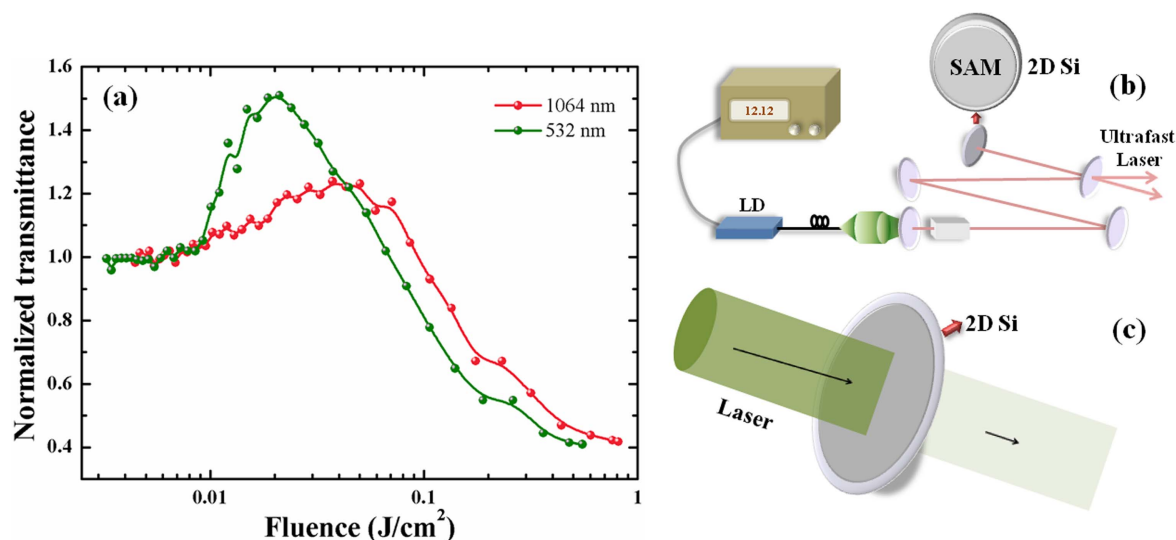


**Figure 5.** (a) Relationship between normalized transmittance and fluence of silicene nanosheets at 1064 and 532 nm with exciting energy of 26.28 and 8.91  $\mu\text{J}$ , respectively, (b) application as saturable absorber in all-solid mode-locked laser, (c) schematic diagram of silicene as OL material.

Because of the two NLA processes, each curve can be divided into three stages, i.e. 1PA, 1PA plus 2PA, 2PA. The threshold of SA induced by 1PA at 1064 nm excitation was 7.8  $\text{mJ cm}^{-2}$ . For 1064 nm excitation, when the excitation intensity varies from 7.8 to 22.9  $\text{mJ cm}^{-2}$ , the SA was the main NLA behavior. When the excitation energy ranged from 22.9 to 54.2  $\text{mJ cm}^{-2}$ , the 1PA and 2PA competed with each other, resulting in the almost stabilized transmittance. When the excitation energy exceeds 54.2  $\text{mJ cm}^{-2}$ , the 2PA occupied the main NLA behavior. For 532 nm excitation, the three stages are corresponding to the excitation energy of 5.9–14.9  $\text{mJ cm}^{-2}$ , 14.9–25.9  $\text{mJ cm}^{-2}$  and beyond 25.9  $\text{mJ cm}^{-2}$ , respectively. Comparing to 1064 nm excitation, the competition stage (14.9–25.9  $\text{mJ cm}^{-2}$ ) between 1PA and 2PA with 532 nm excitation is relatively short. One reason is the stronger linear absorption at 532 nm excitation. Large absorption indicates large vitality of electron at 532 nm wavelength. The second reason is that the single photon energy of 532 nm wavelength is twice as much as that of 1064 nm wavelength. The electrons in valence band are more easier to be stimulated to conduction band with large photon energy excitation, which exhibits the strong 1PA and 2PA absorption. When the 1PA and 2PA absorption are both strong, the competition stage between 1PA and 2PA will be relatively shortened. Due to the lower 1PA threshold and larger OL modulation depth at 532 nm excitation, the silicene nanosheets own much excellent NLA property in short wavelength waveband. Besides, this results illustrate that silicene can be agilely selected as SA material or OL material through appropriately controlling the laser excitation density. The former can be used as saturable absorber in passively Q-switched or mode-locked pulse lasers. The latter has potential applications in protecting human eye or sensitive optical component from laser-induced damage. Figure 5(b) represents the application of silicene as saturable absorber for ultrafast laser in all-solid passively mode-locked laser.

Figure 5(c) is a schematic diagram for the OL application of silicene. Our results demonstrate that silicene is potential 2D NLA material for broadband laser emissions especially in visible waveband.

The relevant research of silicene on damage threshold was relatively rare, but the damage threshold of silicon was researched. Due to the heights of our nanosheets being in the range of 4.5–8.5 nm, i.e. around 14–27 layers (non-monolayer), the damage threshold of our silicene nanosheets must be close to that of silicon, rather than other materials, such as graphene (even in the same group IVA element with the same structure). The damage threshold at 10 ps pulse width and 1064 nm wavelength was 0.78  $\text{J cm}^{-2}$  [37]. According to [37, 38], the damage threshold increased with the growth of the laser pulse width and the decrease of the laser wavelength. Our exciting pulse widths were 40 and 30 ps with wavelengths of 1064 and 532 nm. Compared to [37], the damage threshold would be larger in our experimental condition. In our nonlinear experiment, the maximal exciting energy was 0.81  $\text{J cm}^{-2}$ , which is close to the value (0.78  $\text{J cm}^{-2}$ ). In addition, in contrast to [37, 38], the nanosheets had a small height and were dispersed in ethanol, which intensively decreased the thermal damage of the sample. So the damage threshold of our nanosheets in dispersion liquid would be much larger than 0.78  $\text{J cm}^{-2}$ . Therefore, we can approximately consider that no potential damage occurred to the silicene nanostructure.

## 5. Discussion

The law of  $dI/dL = -\alpha(I)I$  is the absorption properties, where  $\alpha$  is the absorption coefficient and  $L$  is the light traveling distance. The normalized transmittance in the  $z$ -scan

measurement can be expressed as follows [39]

$$T(z) = \sum_{m=0}^{\infty} \frac{\left( \frac{-\alpha_0 L_{\text{eff}}}{1 + z^2/z_0^2} \right)^m}{m+1}, \quad (1)$$

where  $I_0$  is the peak energy intensity at the focus ( $z = 0$ ),  $z$  and  $z_0$  are sample position and the laser Rayleigh length, respectively.  $L_{\text{eff}} = [1 - \exp(-\alpha_0 L)]/\alpha_0$  is the effective length,  $\alpha_0$  is the linear absorption coefficient,  $L = 2$  mm is the sample length. For a system where SA and OL behavior coexist, the total absorption  $\alpha(I)$  is described as  $\alpha(I) = \alpha_0/(1 + I_z/I_s) + \beta I$ , where  $\beta$  is the 2PA coefficient and  $I_s$  are the saturable intensity, defined as the optical intensity when the optical absorbance is reduced to one half of its unbleached value. The first and the second terms on the right side of  $\alpha(I)$  represent the SA and the 2PA, respectively. The excitation intensity  $I_z$  on the optical path is expressed as  $I_z = I_0/(1 + z^2/z_0^2)$ . As presented in part 3,  $\alpha_0$  of silicene nanosheets at 1064 and 532 nm are  $6.5$  and  $7.5 \text{ cm}^{-1}$ , respectively.

The fitted results based on equation (1) are shown in figure 5. The fitted  $I_s$  and  $\beta$  of 1064 and 532 nm are  $54.1 \text{ GW cm}^{-2}$  and  $3.0 \text{ cm GW}^{-1}$ ,  $6.9 \text{ GW cm}^{-2}$  and  $4.8 \text{ cm GW}^{-1}$ , respectively. The lower saturable intensity and higher 2PA coefficient at 532 nm excitation signify the stronger nonlinear properties of silicene at short wavelength condition.

The NLA mechanism of silicene nanosheets is similar to phosphorene [40]. When the excitation energy reaches the threshold of SA, 1PA occurs. The electron at the valence band absorbs the photon and jumps into the conduction band. Due to the constraint of the Pauli exclusion principle, the excited electrons were cooled down. When the excitation energy exceeds the saturable intensity, the redundant photons will transparently pass through. With the excitation energy further increasing, one electron will simultaneously absorb two photons and be stimulated into higher energy levels, which leads to a rapid decline of transmittance, i.e. the OL behavior. According to our results, the superior NLA behavior at 532 nm indicates the smaller energy band volume and lower saturable energy levels at the visible waveband.

The cross-section of 2PA ( $\sigma_{2\text{PA}} = \hbar\omega\beta/N_0$ , where  $\hbar\omega$  is the excitation photon energy and  $N_0 \approx 1.1 \times 10^{18} \text{ cm}^{-3}$  is the density of silicene nanosheets) are calculated to be  $5.1 \times 10^{-46}$  and  $1.6 \times 10^{-45} \text{ cm}^4 \text{ s photon}^{-1}$  for 1064 and 532 nm excitation, respectively. The imaginary part of the third-order nonlinear susceptibility,  $\text{Im}\chi^{(3)}$ , is defined as equation (2), where  $c$  is the vacuum light speed,  $n_0$  is the linear refractive index and  $\omega$  is the angular frequency of the excitation light. The figure of merit (FOM) of the third-order optical nonlinearity is expressed as  $\text{FOM} = |\text{Im}\chi^{(3)}/\alpha_0|$ . Referencing above results,  $\text{Im}\chi^{(3)}$  and FOM of silicene with 1064 and 532 nm excitations are calculated to be  $4.6 \times 10^{-5} \text{ esu}$  and  $9.9 \times 10^{-16} \text{ m}^4 (\text{sW})^{-1}$ ,  $3.7 \times 10^{-5} \text{ esu}$

and  $6.9 \times 10^{-16} \text{ m}^4 (\text{sW})^{-1}$ , respectively

$$\text{Im}\chi^{(3)} = \frac{c^2 n_0^2}{240 \pi^2 \omega} \beta (\text{m W}^{-1}). \quad (2)$$

The same 2D nanosheets exhibit large differences on NLA behavior due to the different excitation conditions, such as excitation pulse width, wavelength, laser facula area and sample concentration [23]. So we compared the NLA properties of other 2D materials in the similar experimental conditions. The saturable intensities of N-G and GO are lower than silicene [20, 41]. But silicene nanosheets owns larger 2PA coefficient than N-G, GO and OH-BN [20, 41, 42]. At the same time, the silicene nanosheets possess larger NLA cross-section than OH-BN [42]. Comparing to other 2D materials, such as OH-BN, the narrow band gap and high flexible electron mobility of silicene benefit the electron transition from valence band to conduction band, which leads to the relatively large NLA coefficient and cross-section. In a word, silicene nanosheets are an exciting NLA material and have potential application in ultrafast lasers and OL devices.

## 6. Conclusion

The silicene nanosheets were exfoliated from the bulk silicon crystal using the LPE method assisted with sonication. The heights of silicene are in the range of 4.5–8.5 nm. An open-aperture Z-scan equipment was used to research the NLA properties of silicene nanosheets. Silicene nanosheets exhibit strong SA and OL behavior. The low saturable intensity and large 2PA coefficient indicate that silicene nanosheets are a promising saturable absorber and OL material, especially for visible lasers.

## Acknowledgments

This work was supported by the National Natural Science Foundation of China (Grant Nos. 11704227, 11304184), the Natural Science Foundation of Shandong Province (ZR2017MF031) and the Scientific Research Foundation of Shandong University of Technology (4041/416033).

## ORCID iDs

Fang Zhang  <https://orcid.org/0000-0002-7132-3144>  
Mengxia Wang  <https://orcid.org/0000-0002-0143-5087>

## References

- [1] Du X, Skachko I, Barker A and Andrei E Y 2008 *Nat. Nano* **3** 491–5
- [2] Novoselov K S, Geim A K, Morozov S V, Jiang D, Zhang Y, Dubonos S V, Grigorieva I V and Firsov A A 2004 *Science* **306** 666–9

- [3] Ataca C, Şahin H and Ciraci S 2012 *J. Phys. Chem. C* **116** 8983–99
- [4] Rubén M B, Cristina G N, Julio G H and Félix Z 2011 *Nanoscale* **3** 20
- [5] Castellanos Gomez A et al 2014 *2d. Mater.* **1** 025001
- [6] Churchill O H H and Pablo J H 2014 *Nat. Nanotechnol.* **9** 330–1
- [7] Choi S, Kwon T and Coskun A 2017 *Science* **357** 279–83
- [8] Zhang Y C, You Y and Xin S 2016 Rice husk-derived hierarchical silicon/nitrogen-doped carbon/carbon nanotube spheres as low-cost and high-capacity anodes for lithium-ion batteries *Nano Energy* **25** 120–7
- [9] Ryu J, Hong D and Choi S 2016 *ACS Nano* **10** 2843–51
- [10] Sychugov I, Valenta J and Linnros J 2017 *Nanotechnology* **28** 072002
- [11] Zamfir M R, Nguyen H T and Moyen E 2013 *J. Mater. Chem. A* **1** 9566–86
- [12] Scalise E and Houssa M 2017 *Nano Res.* **10** 1697–709
- [13] Vogt P, Padova P D, Quaresima C, Avila J, Frantzeskakis E, Asensio M C, Resta A, Ealet B and Lay G L 2012 *Phys. Rev. Lett.* **108** 155501
- [14] Feng B, Ding Z, Meng S, Yao Y, He X, Cheng P, Chen L and Wu K 2012 *Nano Lett.* **12** 3507–11
- [15] Chiappe D, Grazianetti C, Tallarida G, Fanciulli M and Molle A 2012 *Adv. Mater.* **24** 5088–93
- [16] Meng L et al 2013 *Nano Lett.* **13** 685–90
- [17] Fleurence A, Friedlein R, Ozaki T, Kawai H, Wang Y and Takamura Y Y 2012 *Phys. Rev. Lett.* **108** 245501
- [18] Lu Z, Zhu J, Sim D, Zhou W, Shi W, Hng H H and Yan Q 2011 *Chem. Mater.* **23** 5293–5
- [19] Kim S W, Lee J, Sung J H, Seo D, Kim I, Jo M, Kwon B W, Choi W K and Choi H J 2014 *ACS Nano* **8** 6556–62
- [20] Zhang X L, Liu Z B, Li X C, Ma Q, Chen X D, Tian J G, Xu Y F and Chen Y S 2013 *Opt. Express* **21** 7511
- [21] Kumbhakar P, Kole A K, Tiwary C S, Biswas S, Vinod S, Tijerina J T, Chatterjee U and Ajayan P M 2015 *Adv. Opt. Mater.* **3** 828–35
- [22] Wang K, Feng Y, Chang C, Zhan J, Wang C, Zhao Q, Coleman J N, Zhang L, Blau W J and Wang J 2014 *Nanoscale* **6** 10530
- [23] Zhang F, Han S, Liu Y, Wang Z and Xu X 2015 *Appl. Phys. Lett.* **106** 091102
- [24] Feng M, Zhan H B and Chen Y 2010 *Appl. Phys. Lett.* **96** 033107
- [25] Guo Z et al 2015 *Adv. Funct. Mater.* **25** 6996–7002
- [26] Chen Y et al 2015 *Opt. Express* **23** 12823
- [27] Song Y et al 2017 *2d. Mater.* **4** 045010
- [28] Zhao G, Han S, Wang A, Wu Y, Zhao M, Wang Z and Hao X 2015 *Adv. Funct. Mater.* **25** 5292–9
- [29] Gibaja C et al 2016 *Angew. Chem.* **128** 1–6
- [30] Bonaccorso F and Sun Z 2014 *Opt. Mater. Express* **4** 63–78
- [31] Scalise E et al 2014 *Appl. Surf. Sci.* **291** 113–7
- [32] Sirenko A A, Fox J R, Akimov I A, Xi X X, Ruvimov S and Liliental-Weber Z 2000 *Solid State Commun.* **113** 553–8
- [33] Faraci G, Gibilisco S, Pennisi A R and Faraci C 2011 *J. Appl. Phys.* **109** 074311
- [34] Meier C, Luttjohann S, Kravets V G, Nienhaus H, Lorke A and Wiggers H 2006 *Physica E* **32** 155–8
- [35] Yu X, Xue F, Huang H, Liu C, Yu J, Sun Y and Jung Y 2014 *Nanoscale* **6** 6860–5
- [36] Ryu J, Hong D, Choi S and Park S 2016 *ACS Nano* **10** 2843–51
- [37] Wang X, Shen Z H, Lu J L and Ni X W 2010 *J. Appl. Phys.* **108** 033103
- [38] Agustsson R, Arab E, Murokh A, O'Shea B, Ovodenko A, Pogorelsky I, Rosenzweig J, Solov'yov V and Tilton R 2015 *Opt. Mater. Express* **5** 2835
- [39] Mansoor S B, Said A A, Wei T H, David J H and Stryland E W 1990 *IEEE J. Quantum Electron.* **26** 760
- [40] Zhang F, Wu Z, Wang Z, Wang D, Wang S and Xu X 2016 *RSC Adv.* **6** 20027–33
- [41] Zhang F, Wang Z, Wang D, Wu Z, Wang S and Xu X 2016 *RSC Adv.* **6** 3526–31
- [42] Zhao G, Zhang F, Wu Y, Hao X, Wang Z and Xu X 2016 *Adv. Opt. Mater.* **4** 141–6